

Kinetic equations for desorption

Z. W. Gortel,* H. J. Kreuzer, R. Teshima, and L. A. Turski†

Theoretical Physics Institute, Department of Physics, University of Alberta, Edmonton, Alberta T6G 2J1, Canada

(Received 14 January 1981)

Starting from a set of rate equations for the bound-state occupation functions for gas-solid systems in which the surface potential has many physisorbed bound states, we derive a master equation; its kernel is explicitly calculated for phonon-mediated adsorption and desorption in a Morse potential. We give the equivalent Smoluchowski-Chapman-Kolmogorov equation for which we find the Kramers-Moyal expansion. Identifying van Kampen's large parameter Ω for such gas-solid systems, we establish explicit criteria for the validity of a Fokker-Planck equation.

I. INTRODUCTION

In a series of papers¹⁻³ we have developed a quantum statistical theory of desorption of a gas from the surface of a solid in systems which show physisorption at low coverage. The most recent paper was, in particular, devoted to a study of physisorption in gas-solid systems in which the surface potential, i.e., the net static interaction between the particles of the gas and solid phases, develops many bound states, say, at energies E_0, \dots, E_N , into which gas particles can get trapped. Typical examples are the He-LiF system with four bound states, the He-graphite system with $N=4$, the Xe-W system with $N \sim 200$. To calculate the isothermal desorption time for such systems, we have argued that the occupation numbers n_i of gas particles in the i th bound state of the surface potential are, at low coverage, subject to a set of rate equations

$$\frac{dn_i(t)}{dt} = - \left[R_{ci} + \sum_{\substack{j=0 \\ j \neq i}}^N R_{ji} \right] n_i + \sum_{\substack{j=0 \\ j \neq i}}^N R_{ij} n_j, \quad i=0, \dots, N \quad (1)$$

where R_{ji} is the probability for a transition of a gas particle from the i th into the j th bound state of the surface potential, and R_{ci} is the probability for a transition from the i th bound state into the continuum. In (1) transitions from the gas-particle continuum back into any of the bound states are suppressed, as it seems appropriate for an isother-

mal desorption experiment in which desorbing gas particles are pumped out as fast as possible.

To include continuum-bound-state and continuum-continuum transitions simply rewrite (1) as

$$\frac{dn_i(t)}{dt} = \sum_{i' \neq i} R_{i'i} n_{i'} - \sum_{i' \neq i} R_{i'i} n_i, \quad (2)$$

where the indices i and i' run over all bound states and continuum states of a gas particle in the surface potential. Note that as long as the gas volume is finite, the continuum states are discrete, becoming continuous in the large volume or thermodynamic limit. Rate equations similar to (1) and (2) can be derived under certain simplifying assumptions using methods of nonequilibrium statistical mechanics.

In Ref. 3 we have calculated the transition probabilities R_{ij} and R_{ci} in second-order perturbation theory (Fermi's golden rule) for phonon-mediated adsorption and desorption in a one-dimensional model assuming that the surface potential is adequately represented by a Morse potential

$$V_0(x) = U_0(e^{-2\gamma(x-x_0)} - 2e^{-\gamma(x-x_0)}). \quad (3)$$

To find the connection between the isothermal desorption time t_d and the transition probabilities R_{ji} and R_{ci} we write (1) in matrix notation,

$$\frac{d\vec{n}(t)}{dt} = -\vec{R} \cdot \vec{n}(t), \quad (4)$$

where $\vec{n}(t)$ is the $(N+1)$ -dimensional column matrix with elements $n_0(t), \dots, n_N(t)$, and \vec{R} is the $(N+1) \times (N+1)$ matrix of transition probabilities.

To evaluate the formal solution of (4),

$$\vec{n}(t) = e^{-\vec{R}t} \vec{n}(0), \quad (5)$$

we diagonalize the transition matrix

$$\vec{R} \cdot \vec{e}^{(i)} = \lambda_i \vec{e}^{(i)}, \quad (6)$$

where all eigenvalues λ_i are real and positive and assumed to be ordered $\lambda_0 < \lambda_1 < \dots < \lambda_N$. Equation (5) can now be written

$$\vec{n}(t) = \sum_{i=0}^N f_i e^{-\lambda_i t} \vec{e}^{(i)}, \quad (7)$$

where the f_i 's are determined by inverting the initial conditions

$$n_i(0) = \sum_{j=0}^N f_j e_i^{(j)}, \quad (8)$$

where $e_i^{(j)}$ is the i th component of the j th eigenvector. Note that the $\vec{e}^{(j)}$'s are not orthogonal because \vec{R} is not symmetric.

The total (relative) adsorbate occupancy is given by

$$\frac{N(t)}{N(0)} = \sum_{i=0}^N \frac{n_i(t)}{N(0)} = \sum_{i=0}^N S_i e^{-\lambda_i t}, \quad (9)$$

where

$$N(0) = \sum_{l=0}^N n_l(0)$$

and

$$S_i = \sum_{l=0}^N \frac{n_l(0)}{N(0)} \tilde{e}_l^{(i)} \sum_{k=0}^N e_k^{(i)}, \quad (10)$$

where $\tilde{e}_l^{(i)}$ is determined such that

$$\sum_{l=0}^N \tilde{e}_l^{(i)} e_l^{(j)} = \delta_{ij}. \quad (11)$$

Writing (9) as

$$\frac{N(t)}{N(0)} = S_0 e^{-\lambda_0 t} \left[1 + \sum_{j=1}^N \frac{S_j}{S_0} e^{-(\lambda_j - \lambda_0)t} \right], \quad (12)$$

we see that for times $t \gg (\lambda_j - \lambda_0)^{-1}$ for $j=1, \dots, N$ all transients have died out and the time evolution can be characterized by a single time scale

$$t_d = \lambda_0^{-1} \quad (13)$$

provided that S_0 is not substantially smaller than any of the S_j for $j > 0$, which is borne out by our numerical examples. Also note that $\sum_{j=0}^N S_j = 1$. Under these conditions the mean first passage

time^{4,5}

$$\bar{t} = \int_0^\infty \frac{N(t)}{N(0)} dt = \sum_i S_i \lambda_i^{-1} \quad (14)$$

reduces to (13).

Experimentally determined desorption times are usually parametrized over limited temperature regions by a Frenkel-Arrhenius formula

$$t_d = t_d^0 e^{Q/k_B T} \quad (15)$$

where the prefactors t_d^0 typically vary for physisorbed gases from 10^{-7} sec for helium desorbing from Constantan⁶ to 10^{-14} – 10^{-15} sec for xenon desorbing from tungsten.⁷ The heat of adsorption Q/k_B varies from 30 K for the He-Constantan to 4662 K for the Xe-W system. In the microscopic theory of physisorption kinetics it turns out that the depth U_0 of the surface potential (3) is slightly larger than Q , and that its range γ^{-1} determines the prefactor t_d^0 . A smaller range γ^{-1} implies a stronger coupling of the gas particle trapped in a bound state of the surface potential to the phonon bath of the solid, increasing the probability for adsorption of a phonon and thus decreasing t_d^0 . However, reducing the range γ^{-1} of the surface potential keeping its depth U_0 fixed also implies that the number of bound states is reduced so that the number of channels through which the adsorbed particle can cascade up and down the bound states of the surface potential is reduced, leading to a decrease in the desorption rate compensating the increase caused by the stronger coupling to the phonons. One thus finds for the desorption kinetics in gas-solid systems with many surface bound states that details of the surface potential are less important than they are in systems with only a few surface bound states.

As the number of bound states in the surface potential becomes large, it seems plausible to approximate the system of many discrete bound states by a quasicontinuum ranging from the bottom ($-U_0$) of the surface potential well to zero. Whereas in the original system the adatom cascades through a series of discrete bound states, it now performs a random walk through the quasicontinuum of bound-state energies. Such a picture assumes, however, that the adatom can be treated as a classical particle. This, indeed, seems reasonable, e.g., for the Xe-W system, which we will from now on take as the prototype of a gas-solid system that develops many bound states, as the de Broglie wavelength $\lambda_{dB} = [2m(E + U_0)]^{1/2}/\hbar$ of a Xe atom in the lowest bound state of the Xe-W surface

potential is about 0.1 of its range, and it is about 10^{-2} of its range at $E=0$.

To quantify the picture emerging from this discussion we will in Sec. II A perform the continuum limit on the system of rate equations (2) to obtain a master equation. The latter will then be rewritten in Sec. II B as a Smoluchowski-Chapman-Kolmogorov equation, which in turn will be developed into a Kramers-Moyal moment expansion.^{8,9} Truncating the latter after two terms yields, in Sec. II C, a Fokker-Planck equation for physisorption kinetics. In Sec. III, we present the kernel of the master equation explicitly as a perspective three-dimensional plot. Numerical examples of its first two moments which enter the Fokker-Planck equation follow next. For weakly coupled gas-solid systems we will develop approximate expressions for the moments, which will serve to show over which range of potential parameters a simple Boltzmann distribution obtains as an equilibrium solution of the Fokker-Planck equation, thus delineating its range of applicability. The following paper by Kreuzer and Teshima¹⁰ will then be devoted to calculating various approximate desorption and adsorption times starting from the master equation and the Fokker-Planck equation.

An early attempt at a kinetic description of desorption was made by Kramers⁸ who postulated a Langevin equation for the random motion of a classical particle. The interaction of the adsorbed particle with the solid substrate enters this equation as a systematic binding force, a friction force, and a fluctuating force. A microscopic derivation of the Kramers-Langevin equation has recently been attempted by Caroli, Roulet, and Saint-James.¹¹ Simple Langevin-type equations for desorption have also been studied in Refs. 12–15. All of these papers look at the random motion of a classical particle in front of a solid surface. Schaich¹⁶ has recently attempted an appraisal of some of these theories.

In this paper we will study kinetic equations for desorption by following an adsorbed particle in its random walk through the energy levels of the surface potential. Thus our kinetic equations govern the time evolution of the energy distribution function of an adsorbed particle in contrast to the Kramers-Langevin-type equations which determine the spatial distribution functions. An approach similar to ours has been advanced by Pagni and Keck¹⁷ and Pagni¹⁸ who, however, base the microscopic dynamics of the adsorbing particles on a simple classical model, whereas we employ a

quantum-mechanical calculation of phonon-mediated desorption. Yet, we will see, particularly in the following paper, that a number of their conclusions can be verified at least qualitatively in our more refined theory.

II. DERIVATION OF MASTER AND FOKKER-PLANCK EQUATIONS

A. Continuous master equation

For gas-solid systems for which the heat of adsorption Q in (15) is of the order of half an electron volt or more, i.e., for which $Q/k_B \gtrsim 5000$ K, the surface potential, being approximately of depth $U_0 \gtrsim Q$, will develop many bound states, typically a few hundred. In such a situation it seems appropriate to replace sums over i in (1) by integrals over a dimensionless variable which is conveniently chosen to be

$$\epsilon = E/\hbar\omega_D \quad (16)$$

such that for $E=E_i$ being one of the bound-state energies in a Morse potential (3) one gets

$$\epsilon = \epsilon_i = -(\sigma_0 - i - \frac{1}{2})^2/r, \quad (17)$$

where $r = 2m\omega_D/\hbar\gamma^2$ and $\sigma_0^2 = 2mU_0/(\hbar\gamma)^2$. Here $\hbar\omega_D$ is the Debye energy of the solid, which serves as the energy scale for the system. The bound-state occupation functions $n_i(t)$ then go over into $n(\epsilon, t)$ such that

$$n(\epsilon_i, t) = n_i(t). \quad (18)$$

Equation (2) can now be written as

$$\frac{\partial n(\epsilon, t)}{\partial t} = \int_{-u_0}^{\infty} d\epsilon' \rho(\epsilon') W(\epsilon, \epsilon') n(\epsilon', t) - \int_{-u_0}^{\infty} d\epsilon' \rho(\epsilon') W(\epsilon', \epsilon) n(\epsilon, t). \quad (19)$$

where

$$u_0 = \frac{U_0}{\hbar\omega_D} = \frac{\sigma_0^2}{r} = \left[(-\epsilon_0)^{1/2} + \frac{1}{2r^{1/2}} \right]^2 \quad (20)$$

and

$$\rho(\epsilon) = |\epsilon|^{-1/2}. \quad (21)$$

Using the results of Ref. 3 for phonon-mediated transition rates calculated in second-order time-dependent perturbation theory, we get for bound-state-bound-state transitions, i.e., for $-u_0 < \epsilon, \epsilon' < \infty$,

$$\begin{aligned}
W(\epsilon, \epsilon') &= 3\pi r^{1/2} \omega_D \frac{m}{M_s} (\epsilon \epsilon')^{1/2} (\epsilon - \epsilon')^3 \{ \exp[\delta(\epsilon - \epsilon')] \}^{-1} \\
&\times \left[\Theta(1 - \epsilon + \epsilon') \Theta(\epsilon - \epsilon') \frac{\Gamma((ru_0)^{1/2} - (-r\epsilon)^{1/2} + \frac{1}{2}) \Gamma((ru_0)^{1/2} + (-r\epsilon)^{1/2} + \frac{1}{2})}{\Gamma((ru_0)^{1/2} - (-r\epsilon')^{1/2} + \frac{1}{2}) \Gamma((ru_0)^{1/2} + (-r\epsilon')^{1/2} + \frac{1}{2})} \right. \\
&\quad \left. + \Theta(1 - \epsilon' + \epsilon) \Theta(\epsilon' - \epsilon) \frac{\Gamma((ru_0)^{1/2} - (-r\epsilon')^{1/2} + \frac{1}{2}) \Gamma((ru_0)^{1/2} + (-r\epsilon')^{1/2} + \frac{1}{2})}{\Gamma((ru_0)^{1/2} - (-r\epsilon)^{1/2} + \frac{1}{2}) \Gamma((ru_0)^{1/2} + (-r\epsilon)^{1/2} + \frac{1}{2})} \right]. \quad (22)
\end{aligned}$$

where Θ is the step function. Similarly one obtains for bound-state–continuum transitions, i.e., for $-u_0 < \epsilon' < 0$ and $0 < \epsilon < \infty$

$$\begin{aligned}
W(\epsilon, \epsilon') &= \frac{3\pi}{2} r^{1/2} \omega_D \frac{m}{M_s} (-\epsilon \epsilon')^{1/2} \Theta(1 + \epsilon') \Theta(1 + \epsilon' - \epsilon) \{ \exp[\delta(\epsilon - \epsilon')] - 1 \}^{-1} \\
&\times (\epsilon - \epsilon')^3 \frac{\sinh[2\pi(r\epsilon)^{1/2}]}{\sinh^2[\pi(r\epsilon)^{1/2}] + \cos^2[\pi(ru_0)^{1/2}]} \\
&\times \frac{|\Gamma((ru_0)^{1/2} + i(r\epsilon)^{1/2} + \frac{1}{2})|^2}{\Gamma((ru_0)^{1/2} + (-r\epsilon')^{1/2} + \frac{1}{2}) \Gamma((ru_0)^{1/2} - (-r\epsilon')^{1/2} + \frac{1}{2})} \quad (23)
\end{aligned}$$

and for continuum–bound-state transitions

$$\begin{aligned}
W(\epsilon', \epsilon) &= \frac{3\pi}{2} r^{1/2} \omega_D \frac{m}{M_s} (-\epsilon \epsilon')^{1/2} \Theta(1 + \epsilon') \Theta(1 + \epsilon' - \epsilon) (\{ \exp[\delta(\epsilon - \epsilon')] - 1 \}^{-1} + 1) \\
&\times (\epsilon - \epsilon')^3 \frac{\sinh[2\pi(r\epsilon)^{1/2}]}{\sinh^2[\pi(r\epsilon)^{1/2}] + \cos^2[\pi(ru_0)^{1/2}]} \\
&\times \frac{|\Gamma((ru_0)^{1/2} + i(r\epsilon)^{1/2} + \frac{1}{2})|^2}{\Gamma((ru_0)^{1/2} + (-r\epsilon')^{1/2} + \frac{1}{2}) \Gamma((ru_0)^{1/2} - (-r\epsilon')^{1/2} + \frac{1}{2})} \quad (24)
\end{aligned}$$

Note that in (19) the lower integration limit must be taken as the bottom of the surface potential well and not as the lowest bound-state energy, which is slightly larger. Observe that the kernel $W(\epsilon, \epsilon')$ satisfies detailed balance

$$W(\epsilon, \epsilon') e^{-\delta\epsilon'} = W(\epsilon', \epsilon) e^{-\delta\epsilon}, \quad (25)$$

this is not the case for the kernel used in Refs. 17 and 18.

We now want to show that (a) phonon-mediated continuum-continuum transitions vanish for a large system, i.e., as $L \rightarrow \infty$, and (b) that in this limit

$$\frac{\partial n(\epsilon, t)}{\partial t} = 0 \quad \text{for } \epsilon > 0. \quad (26)$$

Recall that (2) is the discrete master equation for a gas in a finite box of length $2L$. From the explicit formulas for a Morse potential, e.g., in Ref. 3, we see that the bound state wave functions of a gas particle are of order 1, i.e.,

$$\phi_i = O(1). \quad (27)$$

The continuum functions ϕ_k are of order $L^{-1/2}$, i.e.,

$$\phi_k = O(L^{-1/2}), \quad (28)$$

so that for bound-state–bound-state transition probabilities we get

$$R_{ii'} = O(1), \quad (29)$$

whereas for bound-state–continuum and continuum–bound-state transition probabilities one finds

$$R_{ki} = O(\lambda/L)$$

and (30)

$$R_{ik} = O(\lambda/L),$$

and for continuum-continuum transitions one finds

$$R_{kk'} = O((\lambda/L)^2), \quad (31)$$

where $\lambda = \gamma^{-1}$ is the range of the surface potential. Next note in (2) that for $\iota = i$ belonging to the bound-state spectrum, the terms with R_{ki} and R_{ik} on the right-hand side still involve a sum over k , so that

$$\sum_k R_{ki} n_i = O(1)$$

and

$$\sum_k R_{ik} n_k = O(1).$$

These are the terms, in addition to the bound-state-bound-state transitions, that have been included in (19).

Next look at those equations in (2) with $\iota = k$ belonging to the continuum. The terms with bound-state-continuum transitions on the right-hand side now involve sums over bound states, i.e.,

$$\sum_i R_{ki} n_i = O\left(\frac{\lambda}{L}\right)$$

and

$$\sum_i R_{ik} n_k = O\left(\frac{\lambda}{L}\right),$$

whereas continuum-continuum transitions contribute terms

$$\sum_{k'} R_{k'k} n_k = O\left(\frac{\lambda}{L}\right)$$

and

$$\sum_{k'} R_{kk'} n_{k'} = O\left(\frac{\lambda}{L}\right),$$

so that

$$\frac{dn_k(t)}{dt} = O\left(\frac{\lambda}{L}\right),$$

which yields (26) in the limit $L \rightarrow \infty$.

To understand this result, consider a gas-solid system in which the surface potential does not develop any bound states. In this case gas particles, scattering elastically and inelastically in the surface potential, can undergo continuum-continuum transitions only. The latter being of order λ/L implies that the time required for a gas to thermalize with the wall would increase like L with the size of the system, that is in the absence of two-body collisions in the gas phase, which we neglected in our model, treating the gas as ideal. This assumption obviously puts restrictions on the gas-solid systems that can be described by the model as given by (2). To get a reasonable description of the adsorption process, collisions in the gas must be so frequent that gas particles undergoing phonon-mediated continuum-bound-state transitions must be replaced from regions in the gas phase further away from the wall in a time short compared to the adsorption time. To describe isothermal desorption with (2) gas particles leaving the bound states must be removed (pumped out) on a time scale faster than the desorption time. We will assume from now on that such situations prevail, in which case (19) and (26) constitute our master equations in the continuum limit.

We intend in the following to derive from (19) an approximate differential equation of the Fokker-Planck type. An accepted procedure entails expanding the integrals in (19) into a Kramers-Moyal expansion.^{8,9} Because our variables ϵ and ϵ' are confined to the semifinite interval $[-u_0, \infty]$, and due to the appearance of the weight $\rho(\epsilon)$ in the integrals, this expansion is not as straightforward as it is on an infinite interval $[-\infty, \infty]$ and with $\rho(\epsilon) = 1$ due to the intermittent appearance of surface terms when carrying out the necessary partial integrations in the Kramers-Moyal expansion. We therefore prefer the somewhat longer, but safer procedure to first establish the Smoluchowski-Chapman-Kolmogorov equation in Sec. II B which is subsequently expanded to yield the differential equation for (19).

B. Smoluchowski-Chapman-Kolmogorov equation

The set of rate equations (2) implies that the motion of an adatom in the surface potential is a random walk through the energy levels and can therefore be described by a Markovian stochastic process. We now want to derive an approximation for the integral operators in (19) in terms of differential operators, i.e., find a Fokker-Planck equation. Following standard procedure^{19,20} we define a propagator $g(\epsilon, t; \epsilon', t')$ for the random walk by

$$n(\epsilon, t) = \int_{-u_0}^{\infty} d\epsilon' g(\epsilon, t; \epsilon', t') n(\epsilon', t').$$

For small time increments $\Delta t = t - t'$ the propagator $g(\epsilon, t + \Delta t; \epsilon', t)$ can be related to the kernel $W(\epsilon, \epsilon')$ of the master equation (19) by

$$g(\epsilon, t + \Delta t; \epsilon', t) = \delta(\epsilon - \epsilon') + \Delta t \left[\rho(\epsilon') W(\epsilon, \epsilon') - \delta(\epsilon - \epsilon') \int_{-u_0}^{\infty} d\epsilon'' \rho(\epsilon'') W(\epsilon'', \epsilon') \right]. \quad (39)$$

One checks easily that by inserting (39) in (38) and taking the limit $\Delta t \rightarrow 0$ we recover (19). $g(\epsilon, t; \epsilon', t')$ itself satisfies the Smoluchowski-Chapman-Kolmogorov equation for $t' \leq t'' \leq t$:

$$g(\epsilon, t; \epsilon', t') = \int_{-u_0}^{\infty} d\epsilon'' g(\epsilon, t; \epsilon'', t'') g(\epsilon'', t''; \epsilon', t'). \quad (40)$$

To derive an expansion of the right-hand side in terms of differential operators we multiply (40) by $\rho(\epsilon)$ and a test function $\tau(\epsilon)$ which is infinitely differentiable on the interval $[-u_0, \infty]$ and vanishes at its endpoints. After integration with respect to ϵ we get

$$\int \tau(\epsilon) \rho(\epsilon) g(\epsilon, t; \epsilon', t') d\epsilon = \int \rho(\epsilon) \tau(\epsilon) g(\epsilon, t; \epsilon'', t'') g(\epsilon'', t''; \epsilon', t') d\epsilon d\epsilon''. \quad (41)$$

On the right-hand side we expand

$$\tau(\epsilon) = \sum_{n=0}^{\infty} \frac{1}{n!} (\epsilon - \epsilon'')^n \tau^{(n)}(\epsilon'') \quad (42)$$

and get after using (40)

$$\begin{aligned} \sum_{n=0}^{\infty} \frac{1}{n!} \int d\epsilon'' \int d\epsilon \rho(\epsilon) (\epsilon - \epsilon'')^n g(\epsilon, t; \epsilon'', t'') g(\epsilon'', t''; \epsilon', t') \tau^{(n)}(\epsilon'') \\ = \int d\epsilon \rho(\epsilon) \tau(\epsilon) g(\epsilon, t; \epsilon', t') + \Delta t \sum_{n=1}^{\infty} \frac{1}{n!} \int d\epsilon'' \tilde{\alpha}_n(\epsilon'') g(\epsilon'', t; \epsilon', t') \tau^{(n)}(\epsilon''), \end{aligned} \quad (43)$$

where for small time intervals $\Delta t = t - t''$, we define moments for $n \geq 1$

$$\tilde{\alpha}_n(\epsilon'') = \frac{1}{\Delta t} \int_{-u_0}^{\infty} d\epsilon \rho(\epsilon) (\epsilon - \epsilon'')^n g(\epsilon, t + \Delta t; \epsilon'', t) = \rho(\epsilon'') \int_{-u_0}^{\infty} d\epsilon \rho(\epsilon) (\epsilon - \epsilon'')^n W(\epsilon, \epsilon''). \quad (44)$$

n partial integrations of the n th term in (43) give

$$\Delta t \sum_{n=1}^{\infty} \frac{(-1)^n}{n!} \int d\epsilon \tau(\epsilon) \frac{\partial^n}{\partial \epsilon^n} [\tilde{\alpha}_n(\epsilon) g(\epsilon, t + \Delta t; \epsilon', t)]. \quad (45)$$

The term $n=0$ is next taken to the left-hand side of (41). After division by Δt we take the limit $\Delta t \rightarrow 0$ and obtain

$$\int d\epsilon \rho(\epsilon) \tau(\epsilon) \frac{\partial}{\partial t} g(\epsilon, t; \epsilon', t') = \int d\epsilon \rho(\epsilon) \tau(\epsilon) \sum_{n=1}^{\infty} \frac{(-1)^n}{n!} \frac{\partial^n}{\partial \epsilon^n} [\tilde{\alpha}_n(\epsilon) g(\epsilon, t; \epsilon', t')]. \quad (46)$$

Multiplying (46) by $n(\epsilon', t')$ and integrating over ϵ' we get

$$\int d\epsilon \tau(\epsilon) \left[\frac{\partial}{\partial t} [\rho(\epsilon) n(\epsilon, t)] - \sum_{n=1}^{\infty} \frac{(-1)^n}{n!} \frac{\partial^n}{\partial \epsilon^n} [\tilde{\alpha}_n(\epsilon) n(\epsilon, t)] \right] = 0. \quad (47)$$

As this relation must hold for any test function $\tau(\epsilon)$ we conclude that the expression in large parentheses must vanish. Thus we can write (19) in a formally equivalent form, usually referred to as the Kramers-Moyal expansion, as

$$\frac{\partial}{\partial t} [\rho(\epsilon) n(\epsilon, t)] = \sum_{n=1}^{\infty} \frac{(-1)^n}{n!} \frac{\partial^n}{\partial \epsilon^n} [\tilde{\alpha}_n(\epsilon) n(\epsilon, t)] = \sum_{n=1}^{\infty} \frac{(-1)^n}{n!} \frac{\partial^n}{\partial \epsilon^n} [\alpha_n(\epsilon) \rho(\epsilon) n(\epsilon, t)], \quad (48)$$

where

$$\alpha_n(\epsilon) = \rho^{-1}(\epsilon) \tilde{\alpha}_n(\epsilon). \quad (49)$$

C. Fokker-Planck equation

Keeping only the first two terms in (48) we get

$$\begin{aligned} \frac{\partial \rho(\epsilon) n(\epsilon, t)}{\partial t} = & - \frac{\partial}{\partial \epsilon} [\alpha_1(\epsilon) \rho(\epsilon) n(\epsilon, t)] \\ & + \frac{1}{2} \frac{\partial^2}{\partial \epsilon^2} [\alpha_2(\epsilon) \rho(\epsilon) n(\epsilon, t)]. \quad (50) \end{aligned}$$

van Kampen²¹ has explained in great detail the validity of such a truncation, which, he argues, can only be justified systematically after the right-hand side of (48) has been rewritten as a series in a small parameter Ω^{-1} . The latter is introduced by rescaling the time variable

$$t = \Omega \tau \quad (51)$$

and by defining

$$\epsilon = \Omega \phi(t) + \Omega^{1/2} \xi, \quad (52)$$

where $\phi(t)$ describes the macroscopic motion of the particle undergoing the random walk with ξ accounting for its fluctuations. $\phi(t)$ can be shown to satisfy the macroscopic law

$$\frac{d\phi(\tau)}{d\tau} = \alpha_1(\phi(\tau)), \quad (53)$$

whereas (48) reduces in lowest order in $\Omega^{-1/2}$ to a linear Fokker-Planck equation for the rescaled distribution function $P(\xi, \tau) = \rho(\epsilon) n(\epsilon, t)$:

$$\begin{aligned} \frac{\partial P(\xi, \tau)}{\partial \tau} = & - \alpha_1'(\phi(\tau)) \frac{\partial (\xi P)}{\partial \xi} \\ & + \frac{1}{2} \alpha_2(\phi(\tau)) \frac{\partial^2 P}{\partial \xi^2}, \quad (54) \end{aligned}$$

where

$$\alpha_1'(\phi(\tau)) = \left. \frac{d}{d\epsilon} \alpha_1(\epsilon) \right|_{\epsilon = \phi(\tau)} \quad (55)$$

with $\phi(\tau)$ being a solution of (53).

Note that an equation like (53) also follows if we multiply (50) by ϵ and integrate over ϵ . We get observing appropriate boundary conditions

$$\begin{aligned} \frac{d}{dt} \int \epsilon n(\epsilon, t) \rho(\epsilon) d\epsilon \\ = \frac{d}{dt} \bar{\epsilon} = \int_{-u_0}^{\infty} \alpha_1(\epsilon) \rho(\epsilon) n(\epsilon, t) d\epsilon, \quad (56) \end{aligned}$$

Expanding

$$\alpha_1(\epsilon) = \alpha_1(\bar{\epsilon}) + (\epsilon - \bar{\epsilon}) \alpha_1'(\bar{\epsilon}) + \dots, \quad (57)$$

this yields

$$\frac{d}{dt} \bar{\epsilon} \approx \alpha_1(\bar{\epsilon}) \quad (58)$$

plus terms involving the fluctuations around $\bar{\epsilon}$.

The question then arises as to what the large parameter Ω is in our gas-solid system. There seem to be two candidates. Recalling (14) one could argue that

$$\Omega = \exp(\delta u_0).$$

Attractive as this identification is, it is very difficult to make the dependence of $\alpha_n(\epsilon)$ or, in turn, of $W(\epsilon, \epsilon')$ on Ω explicit. However, it can be shown, using perturbation theory (see the following paper by Kreuzer and Teshima¹⁰), that the relaxation time t_d scales for large r for $2\delta u_0/\sigma_0 \gg 1$ as

$$\begin{aligned} t_d \approx \omega_D^{-1} \frac{M_s}{m} \frac{1}{18\pi} r^{3/2} u_0^{-5/2} e^{\delta u_0} \\ = \omega_D^{-1} \frac{M_s}{m} \frac{1}{18\pi} \left[\frac{2mU_0}{\hbar^2 \gamma^2} \right]^{3/2} \left[\frac{U_0}{\hbar \omega_D} \right]^{-4} \exp \left[\frac{U_0}{k_B T} \right], \quad (59) \end{aligned}$$

so that it seems appropriate to identify

$$\Omega = \left[\frac{2mU_0}{\hbar^2 \gamma^2} \right]^{3/2} = \sigma_0^3 = (u_0 r)^{3/2} \quad (60)$$

as the large parameter in our system. For example, for the Xe-W system with $U_0/k_B = 4662$ K and $\gamma = 1$ Å we have $\Omega = 4 \times 10^6$. Gas-solid systems with large Ω are, indeed, those that were termed weakly coupled systems in Ref. 2.²² A connection can also be made between Eq. (50) and Kramers's weak-coupling (small-viscosity) Fokker-Planck equation⁸ by defining an action variable $J/\hbar = 2r[u_0^{1/2} - (-\epsilon)^{1/2}]$ and a frequency $\omega/\omega_D = d\epsilon/d(J/\hbar)$. A detailed discussion is planned to be published elsewhere.

III. NUMERICAL EXAMPLES AND DISCUSSION

In this section we want to illustrate and discuss the results of the previous sections mostly by giving explicit numerical examples. Note that the Debye frequency ω_D and the mass ratio m/M_s are overall factors in all formulas. We choose them here appropriately for the Xe-W system; i.e., we set

$\omega_D = 5.3 \times 10^{13} \text{ sec}^{-1}$ and $m/M_s = 0.714$. In Fig. 1 we display the kernel $W(\epsilon', \epsilon)$ of the master equation (19) plotted as a perspective view over a section of the $(\epsilon + \epsilon', \epsilon - \epsilon')$ plane. (The choice of this coordinate system is dictated by aesthetical considerations and has no physical significance.) The pictures are dominated by the bound-state-bound-state transition matrix elements for $\epsilon + \epsilon' < 0$. In Fig. 1 the transitions up to higher bound states produce the lower peak on the left-hand side. The valley between the down and up

transitions reflects the fact that $W(\epsilon, \epsilon) = 0$ on account of the factor $(\epsilon - \epsilon')^3$ in (22)–(24). To see the bound-state-continuum and continuum-bound-state transitions more clearly we display in Fig. 2 two enlarged sections around the origin $\epsilon = \epsilon' = 0$. Their matrix elements are, indeed, much smaller than those for bound-state-bound-state transitions, implying that during the desorption process the bound-state occupation is reshuffled into a thermal distribution much faster than particles are actually desorbing. This suggests that per-

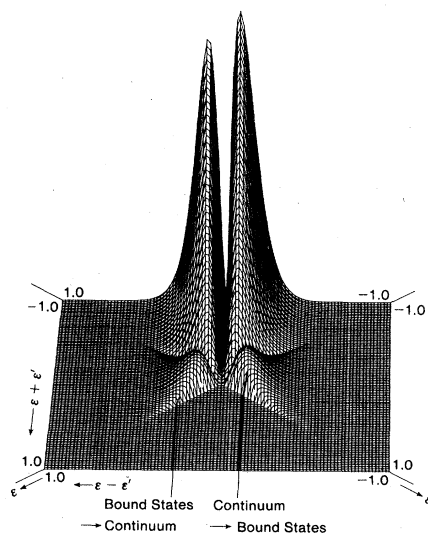
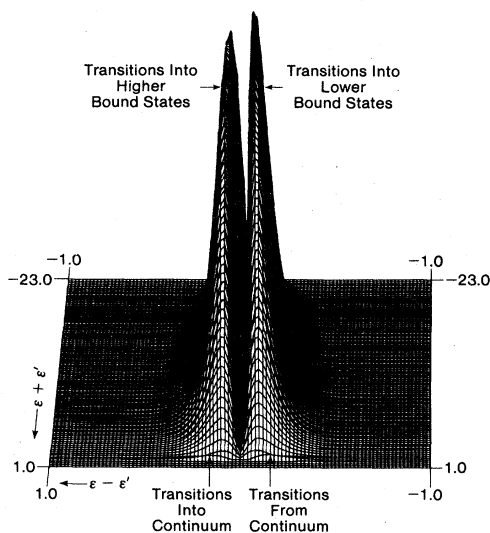
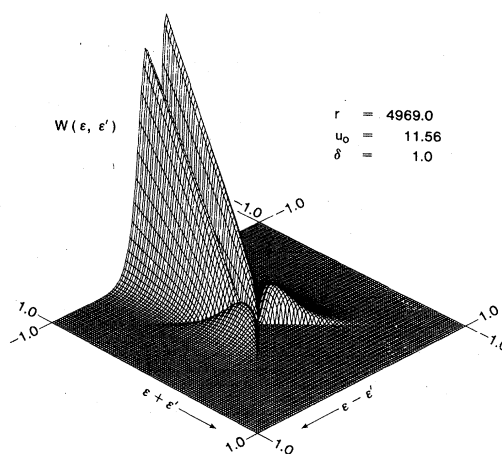
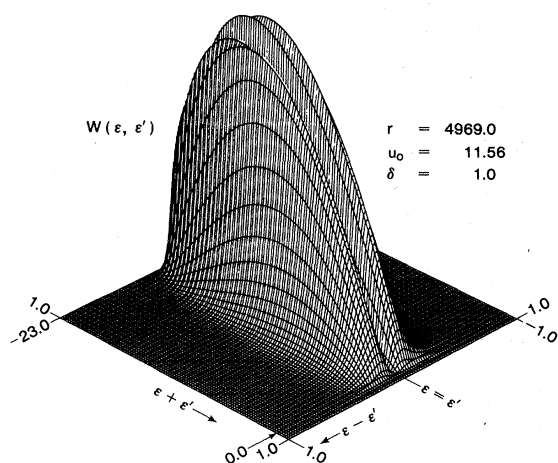


FIG. 1. Perspective views of the kernel $W(\epsilon, \epsilon')$, Eqs. (22)–(24), plotted over the $(\epsilon + \epsilon', \epsilon - \epsilon')$ plane. Note the different scales along the two axes. The highest peaks are $W(\epsilon = -7.385, \epsilon' = -7.315) \omega_D^{-1} M_s/m = 3.4$ and $W(\epsilon = -7.315, \epsilon' = -7.385) = 3.17$. In all numerical examples we chose $m/M_s = 0.714$, $\omega_D = 5.302 \times 10^{13} \text{ sec}^{-1}$.

FIG. 2. Section of Fig. 1 around the origin $\epsilon = \epsilon' = 0$. The maximum in the continuum \rightarrow bound-state transition is $W(\epsilon = -0.07155, \epsilon' = 0.07245) \omega_D^{-1} M_s/m = 0.054$. The maximum in the bound-state \rightarrow continuum transition is $W(\epsilon = 0.07245, \epsilon' = -0.07155) \omega_D^{-1} M_s/m = 0.0466$.

turbation theory advanced in Ref. 10, which leads to the simple expression for the desorption time (59). For increasing temperature the height of all peaks in Figs. 1 and 2 increases because thermalization and desorption become more effective. In addition the up ridge grows with increasing temperature to eventually equal the down ridge for high temperature. The widths of the ridges is quite insensitive to temperature, because it is mainly determined by the gamma functions in (22) except at very low temperature.²³

Let us next turn to a discussion of the ingredients of the Fokker-Planck equation (50). In Fig. 3 we plot the moments $\alpha_1(\epsilon)$, $\tilde{\alpha}_1(\epsilon)$, $\alpha_2(\epsilon)$, and $\tilde{\alpha}_2(\epsilon)$ as calculated from (44) and (49) for $r = 4969.0$, $u_0 = 11.56$, and $\delta = 2$. To understand the role of $\alpha_1(\epsilon)$ in (58) we follow an adparticle whose initial energy is $\bar{\epsilon}_{in} < 0$. Because $\alpha_1(\epsilon) < 0$, $\bar{\epsilon}(t)$ will decrease as a function of time, i.e., the adparticle will loose energy, and move lower into the potential well. Integrating (58) we get

$$t(\bar{\epsilon}) = \int_{\bar{\epsilon}_{in}}^{\bar{\epsilon}} \frac{d\epsilon}{\alpha_1(\epsilon)}, \quad (61)$$

implying that the particle moves fastest where $\alpha_1(\epsilon)$ is largest. But as $\alpha_1(\epsilon)$ goes through zero at about $\epsilon_{min} = -11.2$, the adparticle ceases to loose energy and will stop at the energy, rather than con-

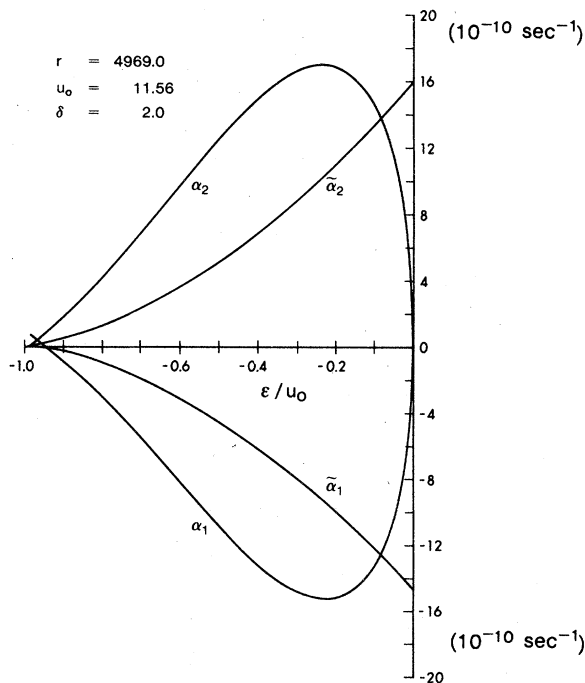


FIG. 3. Moments $\alpha_n(\epsilon)$ and $\tilde{\alpha}_n(\epsilon)$ from (44) and (49).

tinuing down to the bottom of the potential well. It turns out that ϵ_{min} is a strong function of temperature or δ for $\delta \leq 1$ as displayed in Fig. 4, approaching $-u_0$ as $\delta \rightarrow \infty$ or $T \rightarrow 0$, indicating that desorption kinetics based on the Fokker-Planck equation (54) can only be expected to be acceptable for $\delta \geq 1$. For $\delta \leq 1$, i.e., in the high-temperature regime, multiphonon processes, that have been neglected in this theory, will become important, in addition to the expansion (57) becoming dubious.

So far we have only discussed the implications of the macroscopic law (58) on adsorption. Desorption kinetics, on the other hand, must be handled with (50). Note in Fig. 3 that $\alpha_2(\epsilon) \geq |\alpha_1(\epsilon)|$, indicating that higher-order moments in (48) should be kept. For the smaller value $r = 550$ in Fig. 5 the situation is even worse. However, increasing δ to 5 in Fig. 6 reduced $\alpha_2(\epsilon)$ to about half of $|\alpha_1(\epsilon)|$.

We would like to comment briefly on our preference of working with the nonsymmetric kernel (22)–(24) for the master equation. It is well known⁵ that such a kernel satisfying detailed balance (25) can be symmetrized by a transformation

$$S(\epsilon', \epsilon) = e^{\delta\epsilon'/2} W(\epsilon', \epsilon) e^{\delta\epsilon/2}, \quad (62)$$

$$\chi(\epsilon, t) = n(\epsilon, t) e^{\delta\epsilon/2},$$

with no change implied in the above derivation of the Kramers-Moyal expansion, which now reads

$$\frac{\partial}{\partial t} [\rho(\epsilon) \chi(\epsilon, t)] = \sum_{n=1}^{\infty} \frac{(-1)^n}{n!} \frac{\partial^n}{\partial \epsilon^n} \times [\Delta_n(\epsilon) \rho(\epsilon) \chi(\epsilon, t)], \quad (63)$$

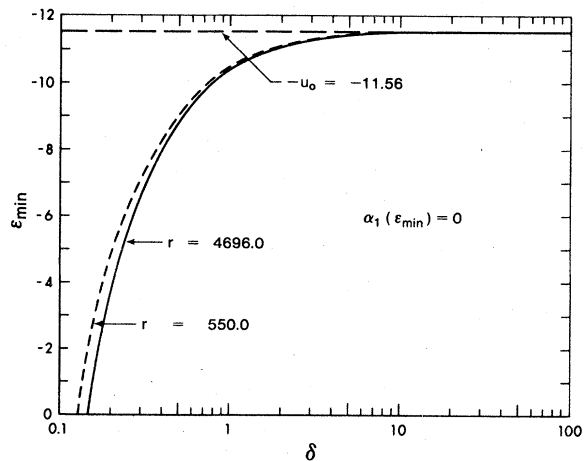


FIG. 4. ϵ_{min} vs δ where $\alpha_1(\epsilon_{min}) = 0$.

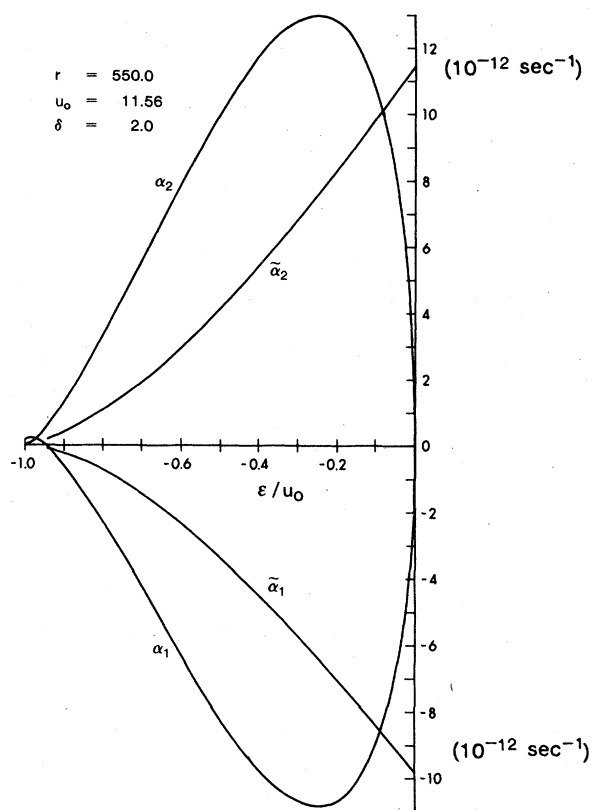


FIG. 5. Moments $\alpha_n(\epsilon)$ and $\tilde{\alpha}_n(\epsilon)$ from (44) and (49).

where

$$\Delta_n(\epsilon) = e^{-\delta\epsilon/2} \rho^{-1}(\epsilon) \times \int d\epsilon' \rho(\epsilon') e^{\delta\epsilon'/2} (\epsilon' - \epsilon)^n W(\epsilon', \epsilon). \quad (64)$$

This symmetrization, of course, changes nothing in the physics of the problem, e.g., (55) or (61) remain unchanged. It turns out that in the numerical examples just given, the exponential under the integral in (64) can be neglected, so that

$$\Delta_n(\epsilon) \approx e^{-\delta\epsilon/2} \alpha_n(\epsilon). \quad (65)$$

with $\alpha_n(\epsilon)$ only weakly dependent on ϵ , the exponential dominates a graph of $\ln \Delta_n(\epsilon)$ vs ϵ (see Fig. 8 of Ref. 17) swamping the dependence on ϵ through $\alpha_n(\epsilon)$. With $\alpha_2(\epsilon)$ being about minus half of $\alpha_1(\epsilon)$ at their respective maxima, one is thus led to conclude¹⁷ that

$$\Delta_1(\epsilon) \approx \frac{1}{2} \frac{\partial \Delta_2(\epsilon)}{\partial \epsilon}, \quad (66)$$

a statement that cannot be made at all between $\alpha_1(\epsilon)$ and $\alpha_2(\epsilon)$ and must be regarded as falsehood construed by the symmetrization (62). Using (66)

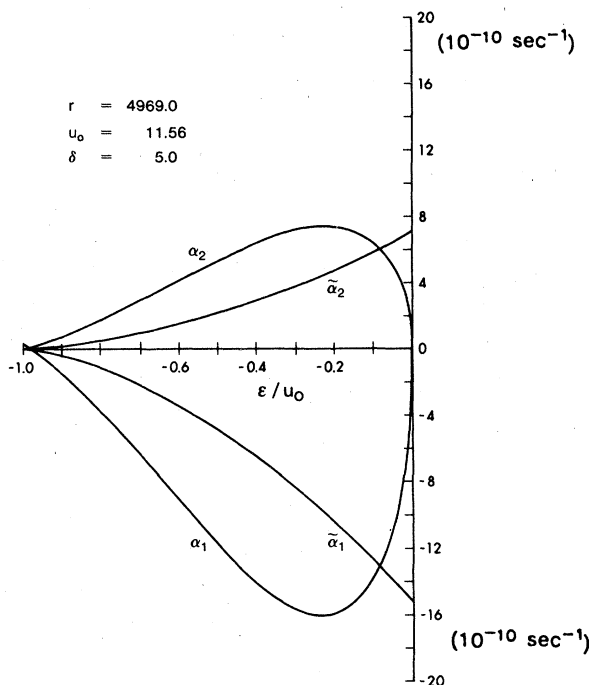


FIG. 6. Moments $\alpha_n(\epsilon)$ and $\tilde{\alpha}_n(\epsilon)$ from (44) and (49).

to simplify the Fokker-Planck equation may introduce errors and is possibly the explanation for the difference between the diffusion and iteration approximations shown in Fig. 10 of Ref. 17.

Recall that the Fokker-Planck equation (50) should be a good kinetic equation for large values of Ω which is proportional to $r^{3/2}$ as seen from (60). We therefore proceed with an asymptotic evaluation of the moments $\alpha_1(\epsilon)$ and $\alpha_2(\epsilon)$ for large r . From Stirling's formula for gamma functions one gets for large x

$$\frac{\Gamma(x+1+a)}{\Gamma(x+1)} \approx x^a \exp\left[\frac{a^2+a}{2x}\right]. \quad (67)$$

Using this in (22) and (23) and approximating in (23)

$$\frac{\sinh[2\pi(r\epsilon)^{1/2}]}{\sinh^2[\pi(r\epsilon)^{1/2}] + \cos^2[\pi(ru_0)^{1/2}]} = 2 + 4 \sum_{n=1}^{\infty} (-1)^n e^{-2\pi n(r\epsilon)^{1/2}} \times \cos[2\pi n(ru_0)^{1/2}],$$

we ultimately get for $\epsilon < 0$ and large r (see the Appendix)

$$\alpha_1(\epsilon) \approx 72\pi\omega_D \frac{m}{M_s} (-r\epsilon)^{1/2} A^{-5} \left[\frac{10B}{\delta A} - 1 \right],$$

$$\alpha_2(\epsilon) \approx 6\pi\omega_D \frac{m}{M_s} (-r\epsilon)^{1/2} A^{-5} \tag{69}$$

$$\times \left[\frac{24}{\delta} + \frac{120\delta}{A^2} - \frac{2520B}{A^3} \right], \tag{70}$$

where

$$A = \left[\frac{r}{u_0} \right]^{1/2} \left[-\frac{u_0}{\epsilon} \right]^{1/2} \tanh^{-1} \left[-\frac{\epsilon}{u_0} \right]^{1/2}, \tag{71}$$

$$B = \frac{1}{4u_0} \left[\frac{r}{u_0} \right]^{1/2} \left[\frac{-u_0}{\epsilon} \right] \times \left[\frac{1}{1+\epsilon/u_0} - \left[-\frac{u_0}{\epsilon} \right]^{1/2} \tanh^{-1} \left[-\frac{\epsilon}{u_0} \right]^{1/2} \right]. \tag{72}$$

Note that for large δ the second terms in $\alpha_1(\epsilon)$ and

in $\alpha_2(\epsilon)$ dominate, whereas for small δ the first terms survive. The approximations (69) and (70) are good for

$$u_0^{1/2} - (-\epsilon)^{1/2} \gg \frac{1}{2r^{1/2}}$$

or

$$u_0 + \epsilon \gg \left[\frac{u_0}{r} \right]^{1/2}, \tag{73}$$

i.e., for $r=4969.0$ and $u_0=11.56$ we need $\epsilon \gg -11.51$; indeed, numerics shows that (69) and (70) are acceptable for $0 > \epsilon > -11$.

We now want to use (69) and (70) to study the equilibrium solution of (50), which satisfies

$$-\frac{\partial}{\partial \epsilon} [\alpha_1(\epsilon)\rho(\epsilon)n_0(\epsilon)] + \frac{1}{2} \frac{\partial^2}{\partial \epsilon^2} [\alpha_2(\epsilon)\rho(\epsilon)n_0(\epsilon)] = 0, \tag{74}$$

with the solution for $\epsilon < 0$,

$$n_0(\epsilon) = e^{\beta\mu} \frac{\alpha_2(0)\rho(0)}{\alpha_2(\epsilon)\rho(\epsilon)} \left[1 - \left[\delta - \frac{d}{d\epsilon} \ln[\alpha_2(\epsilon)\rho(\epsilon)] \right]_{\epsilon=0} + \frac{2\alpha_1(0)}{\alpha_2(0)} \right] \times \int_0^\epsilon d\epsilon' \exp \left[- \int_0^{\epsilon'} \frac{2\alpha_1(\epsilon'')}{\alpha_2(\epsilon'')} d\epsilon'' \right] \exp \left[\int_0^\epsilon d\epsilon' \frac{2\alpha_1(\epsilon')}{\alpha_2(\epsilon')} \right], \tag{75}$$

which matches the free-distribution function

$$n_0(\epsilon) = e^{\beta\mu} e^{-\delta\epsilon}, \quad \epsilon > 0 \tag{76}$$

and its derivative at $\epsilon=0$. The solution (75) simplifies immediately if we note that for moderate δ , such that

$$\frac{5}{3u_0} \ll \delta \ll \left[\frac{2}{5} \frac{r}{u_0} \right]^{1/2}, \tag{77}$$

the second term in (69) and the first term in (70) dominate so that

$$\frac{2\alpha_1(\epsilon)}{\alpha_2(\epsilon)} \approx -\delta \tag{78}$$

for $0 > \epsilon \gg -u_0 + (u_0/r)^{1/2}$. Numerically, (78) seems to be valid for very large r and u_0 values only as we demonstrate with the examples in Figs. 7 and 8. If (78) is a good approximation one also finds that

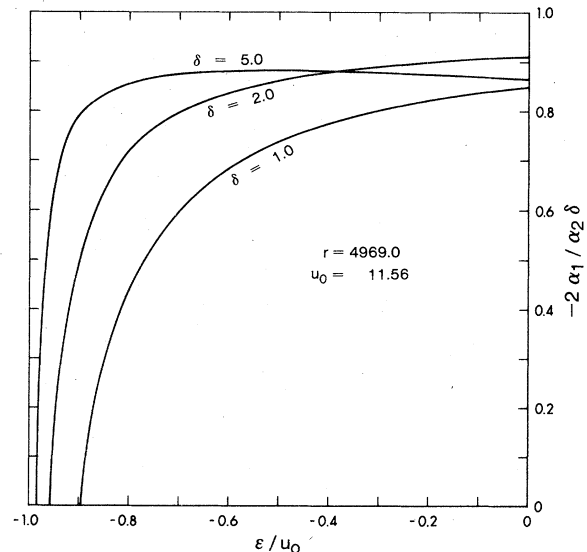


FIG. 7. Ratio $-2\alpha_1(\epsilon)/\alpha_2(\epsilon)\delta$, which must be close to one for the Fokker-Planck equation to be acceptable. Parameters r and u_0 typical for the Xe-W system.

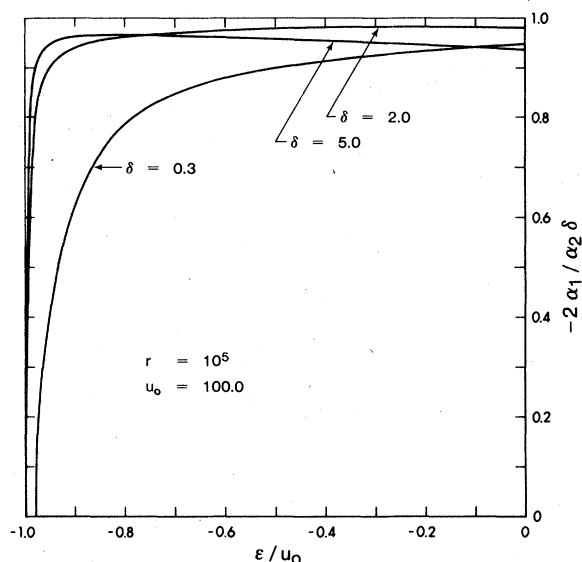


FIG. 8. See Fig. 7. Parameters r and u_0 very large.

$$\left. \frac{\partial}{\partial \epsilon} \ln [\rho(\epsilon) \alpha_2(\epsilon)] \right|_{\epsilon=0} \ll 1 \quad (79)$$

so that (75) reduces to

$$n_0(\epsilon) \approx e^{\beta \mu} \frac{\alpha_2(0) \rho(0)}{\alpha_2(\epsilon) \rho(\epsilon)} e^{-\delta \epsilon}, \quad (80)$$

which, with the further observation that $\alpha_2(\epsilon) \rho(\epsilon)$ varies slowly compared to $\exp(-\delta \epsilon)$ and can thus be approximated by its value at zero, reduces to the Maxwell-Boltzmann distribution

$$n_0(\epsilon) \approx e^{\beta \mu} e^{-\delta \epsilon}. \quad (81)$$

Recall that the original master equation satisfies detailed balance and thus has a Maxwell-Boltzmann distribution as the exact equilibrium solution. The conditions for the validity of (81) are thus necessary for the Fokker-Planck equation (50) to be an acceptable approximation to the master equation (19).

In this paper we have derived from the rate equation (2), a master equation (19) and a Fokker-Planck equation (50), the latter by truncating the Kramers-Moyal expansion (48) for the master equation (19). Numerical examples for the kernel $W(\epsilon, \epsilon')$ of the master equation and for its first two moments $\alpha_1(\epsilon)$ and $\alpha_2(\epsilon)$ led us to approximate expressions for the latter, which in turn allowed us to establish criteria for the validity of the Fokker-Planck equation. They are that the gas-solid system must be weakly coupled, i.e., r must be large, and it must not be at too high a temperature, i.e., Eq. (77):

$$\frac{5}{3u_0} \ll \delta \ll \left[\frac{2}{5} \frac{r}{u_0} \right]^{1/2}.$$

We are now ready to calculate approximate relaxation times for desorption and adsorption from the master equation and the Fokker-Planck equation. This will be done in the following paper by Kreuzer and Teshima.¹⁰

This work was supported in part by the Natural Sciences and Engineering Research Council of Canada.

APPENDIX

We want to derive the approximate expressions (69) and (70) for $\alpha_1(\epsilon)$ and $\alpha_2(\epsilon)$. Starting from (49)

$$\alpha_n(\epsilon) = \int_{-u_0}^{\infty} d\epsilon' \rho(\epsilon') (\epsilon' - \epsilon)^n W(\epsilon', \epsilon) \quad (A1)$$

we split the integral into two parts (a) from $-u_0$ to ϵ where we introduce a new variable $x = \epsilon - \epsilon'$ and (b) from ϵ to ∞ where we introduce $x = \epsilon' - \epsilon$. Note from (22) that $W(\epsilon', \epsilon) = 0$ for $x > 1$ due to the fact that only one-phonon processes are considered. We get with (22) and (23) for $\epsilon < 0$

$$\begin{aligned} \alpha_n(\epsilon) = 3\pi\omega_D \frac{m}{M_s} (-r\epsilon)^{1/2} & \left[\int_0^{\min(1, u_0 + \epsilon)} dx (-x)^{n+3} (e^{-\delta x} - 1)^{-1} \right. \\ & \times \frac{\Gamma((ru_0)^{1/2} + (-r\epsilon)^{1/2} + \frac{1}{2}) \Gamma((ru_0)^{1/2} (-r\epsilon)^{1/2} + \frac{1}{2})}{\Gamma((ru_0)^{1/2} + [r(x - \epsilon)]^{1/2} + \frac{1}{2}) \Gamma((ru_0)^{1/2} - [r(x - \epsilon)]^{1/2} + \frac{1}{2})} \\ & + \int_0^1 dx x^{n+3} (e^{\delta x} - 1)^{-1} \\ & \left. \times \frac{|\Gamma((ru_0)^{1/2} + i[r(x + \epsilon)]^{1/2} + \frac{1}{2})|^2}{\Gamma((ru_0)^{1/2} + (-r\epsilon)^{1/2} + \frac{1}{2}) \Gamma((ru_0)^{1/2} - (-r\epsilon)^{1/2} + \frac{1}{2})} \right], \quad (A2) \end{aligned}$$

where in the second integral we made the replacement

$$\frac{\sinh\{2\pi[r(x+\epsilon)]^{1/2}\}}{\sinh^2\{\pi[r(x+\epsilon)]^{1/2}\} + \cos^2[\pi(ru_0)^{1/2}]} \approx 2. \quad (\text{A3})$$

To simplify the gamma functions we use Stirling's formula,

$$\Gamma(x+1) = (2\pi)^{1/2} x^{x+1/2} e^{-x} \left[1 + \frac{1}{12x} + \dots \right], \quad (\text{A4})$$

and get for $x \gg a$

$$\frac{\Gamma(x+1+a)}{\Gamma(x+1)} \approx x^a \left[1 + \frac{a}{x} \right]^{x+a+1/2} e^{-a} = x^a \exp \left[-a + (x+a+\frac{1}{2}) \ln \left[1 + \frac{a}{x} \right] \right] \approx x^a e^{(a^2+a)/2x}. \quad (\text{A5})$$

This then gives, e.g.,

$$\frac{\Gamma((ru_0)^{1/2} + \frac{1}{2} + [-r(\epsilon+x)]^{1/2}) \Gamma((ru_0)^{1/2} + \frac{1}{2} - [-r(\epsilon+x)]^{1/2})}{\Gamma((ru_0)^{1/2} + \frac{1}{2} + (-r\epsilon)^{1/2}) \Gamma((ru_0)^{1/2} + \frac{1}{2} - (-r\epsilon)^{1/2})} \approx e^{-Ax+Bx^2} \approx e^{-Ax}(1+Bx^2), \quad (\text{A6})$$

where A and B are given in (71) and (72), respectively. Thus we get for (A2)

$$\alpha_n(\epsilon) = 3\pi\omega_D \frac{m}{M_s} (-r\epsilon)^{1/2} \left[(-1)^n \int_0^{\min(1, u_0 + \epsilon)} dx x^{n+3} [(e^{\delta x} - 1)^{-1} + 1] e^{-Ax}(1-Bx^2) + \int_0^1 dx x^{n+3} (e^{\delta x} - 1)^{-1} e^{-Ax}(1+Bx^2) \right]. \quad (\text{A7})$$

Because A is large for large r and u_0 , we can set the upper integration limits as ∞ so that the two integrals can be combined. Because the x integration is limited roughly to $x \lesssim A^{-1} \ll 1$ we can expand the Bose-Einstein factor

$$\frac{1}{e^{\delta x} - 1} \approx \frac{1}{\delta x} - \frac{1}{2} + \frac{\delta}{12} + \dots \quad (\text{A8})$$

Integration then yields the expressions (69) and (70) for $\alpha_n(\epsilon)$.

*Permanent address: Institute of Theoretical Physics, Warsaw University, Warsaw, Poland.

†Permanent address: Institute of Theoretical Physics, Polish Academy of Sciences, Warsaw, Poland.

¹Z. W. Gortel, H. J. Kreuzer, and D. Spaner, *J. Chem. Phys.* **72**, 234 (1980); Z. W. Gortel and H. J. Kreuzer, *Chem. Phys. Lett.* **67**, 197 (1979); Z. W. Gortel, H. J. Kreuzer, and R. Teshima, *Can. J. Phys.* **58**, 376 (1980); H. J. Kreuzer, *Surf. Sci.* **100**, 178 (1980).

²Z. W. Gortel, H. J. Kreuzer, and R. Teshima, *Phys. Rev. B* **22**, 512 (1980); *Chem. Phys. Lett.* **73**, 365 (1980).

³Z. W. Gortel, H. J. Kreuzer, and R. Teshima, *Phys. Rev. B* **22**, 5655 (1980).

⁴E. W. Montroll and K. E. Shuler, *Adv. Chem. Phys.* **1**, 361 (1958).

⁵S. K. Kim, *J. Chem. Phys.* **28**, 1057 (1958).

⁶S. A. Cohen and J. G. King, *Phys. Rev. Lett.* **31**, 703 (1973).

⁷H. J. Dresser, T. E. Madey, and J. T. Yates Jr., *J.*

Chem. Phys. **55**, 3236 (1971); *Surf. Sci.* **42**, 533 (1974).

⁸H. A. Kramers, *Physica* **7**, 284 (1940).

⁹J. E. Moyal, *J. Roy. Stat. Soc. B* **11**, 150 (1949).

¹⁰H. J. Kreuzer and R. Teshima, following paper, *Phys. Rev. B* **24**, 4470 (1981).

¹¹C. Caroli, B. Roulet, and D. Saint-James, *Phys. Rev. B* **18**, 545 (1978).

¹²G. Iche and P. Nozières, *J. Phys. (Paris)* **37**, 1313 (1976).

¹³H. Müller and W. Brenig, *Z. Phys. B* **34**, 165 (1979).

¹⁴S. A. Adelman and J. D. Doll, *J. Chem. Phys.* **61**, 4242 (1974); A. C. Diebold, S. A. Adelman, and Chung Y. Mou, *ibid.* **71**, 3236 (1979); for a review of this approach and additional references see J. D. Doll in *Aerosol Microphysics I. Particle Interaction*, Vol. 16 of *Topics in Current Physics*, edited by W. H. Marlow (Springer, New York, 1980).

¹⁵D. L. Weaver, *Surf. Sci.* **90**, 197 (1979).

¹⁶W. L. Schaich, *J. Phys.* **11**, 2519 (1978).

- ¹⁷P. J. Pagni and J. C. Keck, *J. Chem. Phys.* **58**, 1162 (1973).
- ¹⁸P. J. Pagni, *J. Chem. Phys.* **58**, 2940 (1973).
- ¹⁹S. Chandrasekhar, *Rev. Mod. Phys.* **15**, 1 (1943).
- ²⁰M. Kac and J. Logan, in *Studies of Statistical Mechanics*, edited by E. W. Montroll and J. L. Lebowitz, (North-Holland, Amsterdam, 1979), Vol. VII.
- ²¹N. G. van Kampen, *Can. J. Phys.* **39**, 551 (1961); also see N. G. van Kampen, in *Fluctuations in Solids*, edited by R. E. Burgess (Academic, New York, 1965).
- ²²In Ref. 2 we have calculated the desorption time including all one- and two-phonon processes in fourth-order perturbation theory for a gas-solid system that develops only one bound state at an energy E_0 . Relevant to the discussion here is the observation above Eq. (87) in the first paper of Ref. 2 that a Frenkel-Arrhenius parametrization (15) of the desorption time, calculated in second-order perturbation theory is possible if $k_B T \ll |E_0|$, but not arbitrarily small. This is more or less equivalent to the condition $\delta u_0/\sigma_0 \gg 1$ for the validity of (59) of this paper, because a Morse potential of depth u_0 develops N bound states with $\sigma_0 - \frac{3}{2} < N < \sigma_0 - \frac{1}{2}$, so that u_0/σ_0 is the average spacing between bound states. The numerical verification of this criterion will be given in the following paper by H. J. Kreuzer and R. Teshima (Ref. 10).
- ²³To appreciate the richness of our quantum-mechanical model as compared to a simple classical model, compare Figs. 1 and 2 of this paper with Fig. 6 of Ref. 17. Note that the kernel $R(\epsilon, \epsilon')$ in Ref. 17, as calculated from classical mechanics, does not satisfy the basic requirement of detailed balance and had to be symmetrized. Also note that the kernel $W(\epsilon, \epsilon')$, displayed for our model in Figs. 1 and 2, is chosen as a Gaussian in the difference $\epsilon - \epsilon'$ in Ref. 13. Using (67) one finds that for large r , $W(\epsilon, \epsilon')$ can be approximated by a function of $|\epsilon - \epsilon'|$, with an exponential factor whose argument is linear in $|\epsilon - \epsilon'|$.